Landmark Point-Based Mobile Robot System with IoT Communication for Warehouse Environments

Intan Saragih
School of Electrical Engineering
Telkom University
Bandung, Indonesia
intansaragih@student.telkomuniversity.ac.id

Eduardus Arjuna Herwian
School of Electrical Engineering
Telkom University
Bandung, Indonesia
arjunaherwian@student.telkomuniversity.ac.id

Reinald Mariel
School of Electrical Engineering
Telkom University
Bandung, Indonesia
reinaldm@student.telkomuniversity.ac.id

Rifqi Fathin Syiraz
School of Electrical Engineering
Telkom University
Bandung, Indonesia
rifqisyiraz@student.telkomuniversity.ac.id

Azam Zamhuri Fuadi
School of Electrical Engineering
Telkom University
Bandung, Indonesia
azamzamhurifuadi@telkomuniversity.ac.id

Angga Rusdinar
School of Electrical Engineering
Telkom University
Bandung, Indonesia
anggarusdinar@telkomuniversity.ac.id

***Abstract*—This paper presents a mobile robot system for automated warehouse tasks, utilizing magnetic landmark points for precise navigation and Internet of Things (IoT) communication for efficient data exchange. A 16-element magnetic sensor guides the robot, with central elements detecting the path and outer elements identifying special markers that trigger actions like stopping, charging, or direction changes. An intelligent stopping system allows the robot to skip locations without stop commands. A central cloud-based communication setup, using Google Sheets, enables secure and efficient two-way data exchange between the operator and the robot via HTTPS/TLS and JSON formats. Experimental results show an average success rate of 91.42% for marker detection, with performance variations influenced by speed and marker placement accuracy. The study also analyzes end-to-end communication latency and throughput, highlighting areas for future optimization for real-time capabilities.**

Keywords—Mobile robot, Landmark point, IoT communication, Cloud robotics, Warehouse automation, Magnetic guidance, Data exchange, Latency, Throughput.

I. INTRODUCTION

The industrial sector has widely adopted mobile robots for the automated transfer of raw materials, work-in-progress, and finished goods, aiming for optimal cost and time efficiency, as well as enhancing safety in warehouse environments [1]. These robots, used for material transportation, significantly reduce labor and costs by automating repetitive tasks [2]. Mobile robots exist in various forms, ranging from guided types that follow specific paths to fully autonomous AI-based systems [3]. In this study, a guided path mobile robot system was chosen for its straightforward installation, lower costs, and suitability for defined tasks.

However, precise stopping, dynamic assignment, and real-time monitoring remain challenges in current guided mobile robot systems [4]. This research addresses these by designing, implementing, and evaluating a novel landmark point-based mobile robot system with a versatile, cloud-based Internet of Things (IoT) communication framework. This paper's primary contributions include a magnetic landmark detection system for precise actions, a conditional stopping mechanism, and a centralized IoT communication architecture. A comprehensive analysis of end-to-end communication latency and throughput is also presented. The remainder of this paper details the literature review, followed by implementation and experimental evaluation, and concludes with findings and future research directions.

II. LITERATURE REVIEW

A. Mobile Robot

The industrial sector has widely adopted mobile robots for the automated transfer of raw materials, work-in-progress, and finished goods, aiming for optimal cost and time efficiency [2]. Mobile robots themselves exist in various forms, ranging from guided types that follow specific paths to fully autonomous AI based systems, each tailored to distinct industrial requirements [3]. In this study, a guided path method was selected for investigation. The rationale for this selection includes straightforward installation, lower implementation costs, and high adaptability for operations in confined spaces.

FIGURE 1
3D Design of Mobile Robot

Mobile robots are typically constructed from robust materials, such as steel, to withstand potential impacts and enhance durability within operational environments [5]. However, this inherent durability often results in substantial self-weight, necessitating powerful motors capable of self-propulsion. In this study, the mobile robot is constructed from steel and galvanized plates. It is powered by DC motors designed to pull a payload of up to 500 kg (excluding its own weight). Two DC motors, one on each side, serve as the primary differential drive system, complemented by four caster wheels for support and stability. Differential drive is considered the most suitable choice for a two DC motor primary propulsion system [6].

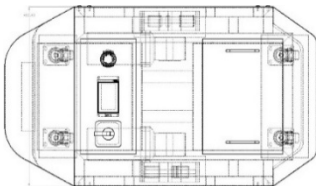

FIGURE 2
Blueprint of Mobile Robot

B. Magnetic Sensor

Magnetic line sensors are crucial for line-following navigation in mobile robots, functioning by detecting magnetic tape's presence and position via Hall effect sensor arrays. These sensors are often preferred for certain applications over infrared (IR) sensors, as IR is susceptible to light and surface interference that compromises accuracy and reliability [7]. This inherent robustness allows magnetic sensors to guide robots with high precision, making them a dependable choice for industrial environments requiring repetitive movements on clear routes, like material transfer robots.

As the sensor array moves over magnetic tape, individual detectors register the magnetic field, allowing the system to determine the line's center and any deviation. This data is processed for precise motion adjustments, ensuring the system stays on its path. The sensor's resilience to dust, dirt, and lighting variations makes it a reliable choice for industrial environments.

FIGURE 3
Magnetic Sensor

The magnetic sensor features 16 configurable elements that detect magnetic field polarity. In this study, 12 central elements are used for straight-line detection and path deviation, while outer elements handle landmark detection. Landmark detection triggers commands such as stopping, charging, or branching. Operating on the Hall effect principle, this sensor accurately detects magnetic field strength and polarity, ensuring precise and stable readings from the magnetic tape guidance path.

C. Landmark Point

In the developed mobile robot system, magnetic landmarks play a crucial role in defining critical operational points, including stop locations, charging stations, and path branching points. These landmarks are composed of segments of the same magnetic tape used for the main guidance line and are strategically positioned directly in front of destination terminals, charging stations, or pathway divergences.

A key feature in this design is an intelligent conditional stopping mechanism. The mobile robot continuously follows its predetermined path until it detects the target landmark. However, the mobile robot will only halt at the destination terminal if and only if there is an active command from the central system to stop at that terminal. Should no relevant stop command exist for the detected terminal landmark, the mobile robot will autonomously bypass that terminal and proceed along its path until it encounters another landmark requiring a specific action (e.g., a landmark for stopping at the next ordered terminal, or a branching landmark). The variations in these landmark patterns are programmable according to user requirements, offering high flexibility in managing routes and mobile robot interactions within the operational environment.

D. Communication System

The fundamental role of a mobile robot's communication system is to facilitate seamless interaction between the robot, its operators, and the broader operational environment. This section reviews various architectural paradigms, communication protocols, and security considerations pertinent to designing robust mobile robot communication systems.

a) Architectural Paradigms in Mobile Robot Communication

Mobile robot communication systems adopt various architectural paradigms. Centralized cloud-based infrastructures offer advantages like offloading computational loads (e.g., SLAM, path planning, image processing) to powerful servers, addressing robot limitations in processing and memory [8], [9]. Cloud instances also enable centralized path planning, resource management, and extensive data logging. However, centralized models can introduce single points of failure and increased latency, especially for local robot-to-robot interactions. Conversely, peer-to-peer protocols like DDS and Zenoh reduce latency and improve resilience for direct device communication at the "edge" [10]. The choice between centralized, decentralized, or hybrid models is crucial, depending on application needs, from remote teleoperation to real-time multi-robot systems [11].

b) Communication Protocols and Data Formats

The selection of communication protocols and data formats is critical for mobile robot systems. Lightweight and readily available web protocols like HTTP, often coupled with data formats such as JSON (JavaScript Object Notation), are commonly employed for their cost-effectiveness and accessibility in cloud-based solutions. JSON, being a relatively lightweight and human-readable data structure, significantly enhances interoperability across various system components. However, the request-response model inherent in HTTP can introduce overhead due to repeated connection establishments or the management of persistent connections for continuous polling. While this might be manageable for asynchronous, non-safety-critical scenarios with moderate update frequencies, mobile robotics applications demanding ultra-low latency, high throughput, or deterministic real-time control (e.g., multi-robot coordination with millisecond precision) often necessitate more specialized communication protocols and data management solutions. These are designed specifically to minimize overhead and ensure timely data delivery [12]. The publish-subscribe (Pub/Sub) messaging model, a core feature of protocols like MQTT, DDS, and Zenoh, effectively decouples publishers from subscribers. This design facilitates dynamic network configurations, simplifies node management, and significantly improves system scalability by allowing many-to-many communication without direct coupling.

c) Security Considerations in Mobile Robot Communication

For web-based robotic interfaces, standard web security practices like HTTPS (HTTP Secure), which encrypts data via TLS/SSL, are crucial for confidentiality and integrity over public networks [13]. Cross-Origin Resource Sharing (CORS) policies are also relevant, often requiring proxy servers for secure communication between different origins. For sensitive or uncontrolled deployments, further enhancements include granular device-level authentication, secure boot processes, and specialized security protocols like ROS 2's DDS-Security or gRPC's built-in TLS. These advanced features offer data integrity, message authentication, and fine-grained access control, essential for scaling robotic systems to more critical applications.

III. RESULTS AND DISCUSSIONS

A. Landmark Points Implementation

Landmark points are precisely positioned at locations where the mobile robot is required to perform specific interventions, including stopping at terminals, accelerating, path selection, and utilizing charging stations. The mobile robot's track area is accessible without spatial limitations, provided Wi-Fi connectivity remains available to the robot. For experimental purposes, the researchers conducted tests on a track spanning 40.2 meters.

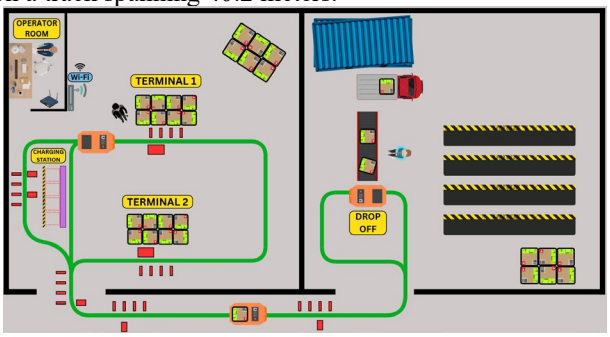

FIGURE 4
Testing Zone

a) Binary Encoding of Landmarks

The mobile robot's magnetic guidance system uses precisely encoded landmarks, made from magnetic tape segments, to trigger operational commands. These landmarks are translated into unique 8-bit binary codes, read by eight specific elements of a 6-element magnetic sensor array. Each 8-bit code is generated from eight distinct magnetic field transitions (rising and falling edges) produced by four physical magnetic segments within the landmark pattern, with each sequential edge contributing one bit to the code.

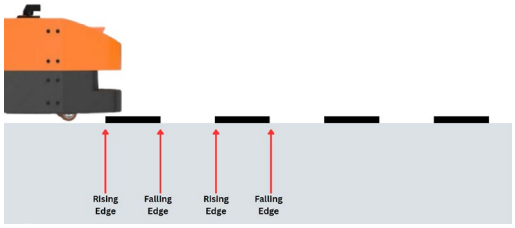

FIGURE 5
Landmark Edge

The assignment of '0' or '1' to each bit is critically determined by the simultaneous detection of a polling signal. Specifically:

- If a rising edge or falling edge from a landmark segment occurs in alignment with an active polling signal from the dedicated polling sensors (located on the right side of the mobile robot's sensor array), the corresponding bit in the 8-bit binary code is set to '0'.
- Conversely, if an edge occurs without alignment with an active polling signal, the bit is set to '1'.

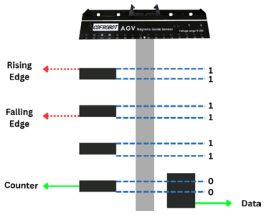

FIGURE 6
Binary Output

Upon completion of the binary encoding process, an 8-bit binary code, such as the example '11111100' mentioned above, is generated for each landmark. This generated binary code then needs to be converted into its decimal equivalent. This decimal value will subsequently serve as the unique command code for each respective landmark. This conversion to a decimal format is crucial as it significantly facilitates the mobile robot's control system in processing, storing, and comparing detected landmarks, thereby enabling quick and efficient execution of specific commands corresponding to the landmark's identity.

Binary numbers can be converted to their decimal equivalents using the formula presented below, starting with B_0 as the rightmost (least significant) bit (1):

$$Decimal = (B_7 \times 2^7) + (B_6 \times 2^6) + (B_5 \times 2^5) + (B_4 \times 2^4) + (B_3 \times 2^3) + (B_2 \times 2^2) + (B_1 \times 2^1) + (B_0 \times 2^0) \quad (1)$$

Presented below are the decimal values derived from the binary codes used. These decimal values serve as unique positional markers and can be programmed to trigger the required operational commands.

TABLE I.
DECIMAL OF BINARY

Position	Binary	Decimal
Terminal 1	11110000	240
Terminal 2	00001111	15
Drop-Off	00111111	63
Speed Up	11001111	243
Normal Speed	11110011	207
Charging Station	00111100	60
Fork	11111100	252

b) Signal Output

To ensure the accurate placement of magnetic landmarks, an oscilloscope can be utilized to verify the synchronization between the polling and interrupting signals. An example of the observed signal is presented below.

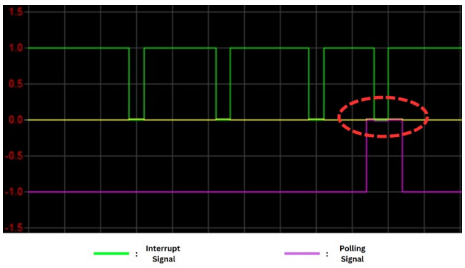

FIGURE 7
Signal Ouput

In every Output Signal graph, both signals will approach '1', indicating that the sensor has detected a magnet in its path. Conversely, the signals will return to '0' when the magnet is no longer detected.

To generate a '1' bit in the binary landmark code, precise temporal synchronization between the interrupt and polling signals is required, as illustrated by the red-circled areas. The specific conditions for generating a '0' bit at each signal transition (edge) are as follows:

- On the rising edge: The polling signal must reach 1 before the interruption signal.
- On the falling edge: The polling signal (purple) must reach 0 after the interrupt signal.

These specific alignment and timing conditions are crucial for accurate encoding. A bit will be '1' if the polling requirement is met during the edge transition, and '0' if it is not.

c) Result of Testing

In this study, seven landmark variations are utilized, each possessing its own unique features. These variations are determined based on specific research requirements, compatibility with field conditions, and the ease of landmark application.

The experimental results evaluatin" the'performance of the magnetic landmark detection and response system in the mobile robot are presented. Each landmark function was tested 20 times, yielding a total of 140 trials. Overall, the landmark system demonstrated a high average success rate of 91.42% (128 out of 140 trials).

TABLE II.
RESULT OF TESTING

Position	# of Experiment	Success	Percentage
Terminal 1	20	20	100%
Terminal 2	20	20	100%
Drop off	20	19	95%
Speed Up	20	18	90%
Normal Speed	20	16	80%
Charging Station	20	17	85%
Fork	20	18	90%
Total	**140**	**128**	
Percentage	**91.42%**		

Test results showed varied landmark performance: Terminal 1 and 2 achieved 100% success, confirming high reliability for primary stopping points. The Drop off function had a 95% success rate (19/20 trials). Speed Up and Fork landmarks each succeeded in 90% of trials (18/20 trials), while the Charging Station reached 85% success (17/20 trials).

Normal Speed landmark recorded the lowest success rate at 80% (16/20 trials), primarily due to the mobile robot's high traversal speed. This high speed makes marker reading more difficult and briefer, impacting the reception of the speed reduction command. The challenge of precise marker placement for high-speed detection also contributes to this reduced success rate.

d) Landmark Positioning

The precise placement of landmarks for both interruption and polling mechanisms plays a crucial role. Imprecise positioning can result in the magnetic sensor failing to correctly detect rising or falling edges. Furthermore, such positioning errors can disrupt the robot's line-following navigation, potentially causing the robot to misinterpret conditions as a turn and execute an undesired change in direction.

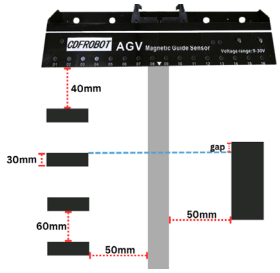

FIGURE 8
Landmark Positioning

For landmark identification, six sensor bits (three on each side) create a 30 mm wide reading area, with the magnetic sensor's working distance being 40 mm. Interrupt magnetic pieces, 40 mm wide and 30 mm long, provide a 10 mm deviation tolerance and are placed in four segments with 60 mm spacing. Polling magnetic pieces, also 40 mm wide, have varied lengths to form binary patterns and must be longer than interrupt signal edges for accurate '1' bit encoding. All interrupt and polling pieces are positioned 50 mm from the main magnetic guideline.

B. Communication System Implementation

The developed system integrates a mobile robot with an online communication infrastructure for remote operations and data exchange. An operator initiates task requests via a Flutter-based web interface, with all system components interconnected through a centralized cloud-based infrastructure. Google Sheets serves as the database, enhanced by Google Apps Script to support HTTP GET/POST protocols, and data is parsed as JSON, enabling real-time bidirectional communication. This centralized setup handles both operator commands (downlink) transmitted from the web interface to the robot, and sensor data (uplink) from the robot, which is stored in Google Sheets and displayed to the operator.

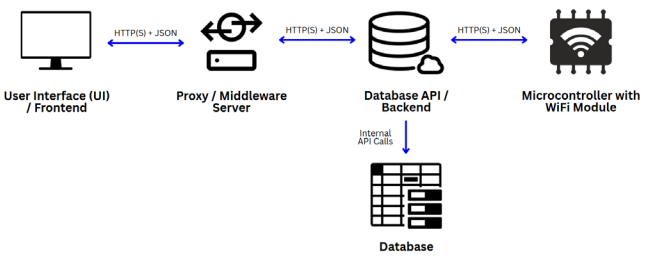

FIGURE 9
Communication System *Architecture of Mobile Robot*

The system's security leverages the Google ecosystem's multi-layered protection, including data encryption (at rest and in transit), robust Identity and Access Management (IAM), and continuous monitoring. Google Sheets is secured via restricted sharing, while the Apps Script web application, acting as the backend API, is configured for custom server-side authorization. Communication among the Flutter web interface, Apps Script backend, and the ESP32-equipped mobile robot is secured via HTTPS/TLS for confidentiality and integrity, with Cross-Origin Resource Sharing (CORS) challenges resolved by a Firebase-based proxy that offers additional validation and URL obfuscation.

TABLE III.
SELECTED PLATFORMS FOR MOBILE ROBOT ONLINE COMMUNICATION ARCHITECTURE

Frontend	Proxy Server	Backend	Database	MCU with WiFi
Flutter Web-app	Firebase Hosting	Apps Script	Google Sheets	ESP32

a) Wireless Communication Link Characterization

The wireless communication link between the mobile robot and the gateway exhibited a clear inverse relationship between Received Signal Strength Indicator (RSSI) and distance, as shown in Table V and the accompanying plot. Signal strength was robust at 0.6m (-3 dBm) but predictably attenuated with increased distance, reaching -67 dBm at the 8.2m "Drop-off" point, indicating practical range limitations. Generally, RSSI values above -70 dBm are considered strong and suitable for reliable data transmission in wireless systems [14]. Low standard deviation values (0.27 to 0.39 dBm) across 20 trials confirmed high signal stability and consistency, suggesting a relatively stable propagation environment. A slight increase in standard deviation at greater distances may be due to environmental factors or noise as signal power diminished.

TABLE IV.
WIRELESS SIGNAL STRENGTH (RSSI) MEASUREMENTS AT VARIOUS MOBILE ROBOT TERMINAL DISTANCES

SSID	CH	Avg. RSSI (dBm)	Std. Dev. (dBm)	Distance to Gateway	Number of Trials
Mobile Robot WiFi	11	-3	0.27	0.6m (Charging Station)	20
		-31	0.33	3.4m (Terminal 1)	
		-26	0.31	3.0m (Terminal 2)	
		-67	0.39	8.2m (Drop-off)	

b) End-to-End Communication Latency Analysis

End-to-end communication latency, from order transmission to mobile robot movement, was analyzed and summarized in Table VI. The average time delay was lower at the "Charging Station" (3.16 s, -3 dBm RSSI) than at the "Drop-off" position (3.28 s, -31 dBm RSSI). This suggests that increased path loss and potential retransmissions in weaker signal environments contribute to higher latency, alongside network transit time. The small data packet size (168 bytes) indicates that network transmission is a factor, but cloud processing overhead and robot execution time also influence total delay. Low standard deviations (0.11 s at Charging Station, 0.16 s at Drop-off) indicate high consistency across 20 trials. A slight variance increase at "Drop-off" is attributed to minor packet retransmissions or processing queue fluctuations due to reduced signal quality. These findings emphasize optimizing cloud and robot processing pipelines, in conjunction with maintaining robust wireless link quality, to further reduce overall latency.

TABLE V.
DOWNLINK LATENCY : ORDER TRANSMISSION TO MOBILE ROBOT MOVEMENT

Position	Avg. RSSI (dBm)	Avg. Time Delay (s)	Std. Dev. (s)	Avg. Data Packet Size (bytes)	Number of Trials
Charging Station	-3	3.16	0.11	168	20
Drop-off	-31	3.28	0.16		

Table VII details the uplink latency, the end-to-end delay from mobile robot sensor data acquisition to web interface display. Average delays ranged from 3.21 s at the Charging Station (-3 dBm RSSI) to 3.58 s at Terminal 2 (-26 dBm RSSI). Unlike downlink, uplink latency generally increased with diminishing signal strength, indicating network transit time's greater role due to signal degradation and retransmissions. Consistency across 20 trials was shown by low standard deviations (0.27 s to 0.35 s), though higher variance at greater distances suggested increased variability. Despite a small 27-byte average data packet size, cumulative network conditions, robot sensor processing delays, and cloud data ingestion/rendering collectively influenced observed uplink latencies. Optimizing these multi-faceted components is crucial for minimizing overall delay in real-time sensor data visualization.

TABLE VI.
UPLINK LATENCY: MOBILE ROBOT SENSOR DATA ACQUISITION TO WEB INTERFACE DISPLAY

Position	Avg. RSSI (dBm)	Avg. Time Delay (s)	Std. Dev. (s)	Avg. Data Packet Size (bytes)	Number of Trials
Charging Station	-3	3.21	0.27	27	20
Terminal 1	-31	3.52	0.33		
Terminal 2	-26	3.58	0.31		
Drop-off	-67	3.53	0.35		

c) Data Throughput Performance

To quantify data throughput, average packet sizes and end-to-end average time delays from Table VI (downlink) and Table VII (uplink) were utilized. The calculated throughput represents the effective end-to-end performance for the entire process (order transmission to robot movement for downlink, and sensor data acquisition to web display for uplink), not solely raw network transfer rates. This holistic measurement accounts for all contributing factors to the observed latency for each direction.

Throughput in bits per second (bps) is calculated by dividing the total data transferred in bits by the time taken for the transfer in seconds, as shown in Equation (1):

$$Throughput\ (bps) = \frac{Total\ Data\ Transferred\ (bits)}{Time\ Taken\ (seconds)} \quad (1)$$

To convert bits per second (bps) to kilobits per second (kbps), the bps value is divided by 1,000, as per Equation (2):

$$Throughput\ (kbps) = \frac{Throughput\ (bps)}{1000} \quad (2)$$

Following this methodology, the average downlink time delay, derived from Table VI, is 3.22 s. The effective downlink throughput is calculated as:

$$Throughput\ (bps)_{downlink} = \frac{1344\ bits}{3.22\ s} \approx 417.39\ bps \quad (3)$$

$$Throughput\ (kbps)_{downlink} = \frac{417.39\ bps}{1000} = 0.417\ kbps \quad (4)$$

Meanwhile, the average uplink time delay, derived from Table VII, is 3.46 s. The effective uplink throughput is calculated as:

$$Throughput\ (bps)_{uplink} = \frac{216\ bits}{3.46\ s} \approx 62.43\ bps \quad (5)$$

$$Throughput\ (kbps)_{uplink} = \frac{62.43\ bps}{1000} = 0.062\ kbps \quad (6)$$

The effective end-to-end throughput values of approximately 0.417 kbps for downlink and 0.062 kbps for uplink highlight a significant bottleneck. These rates are considerably low compared to modern mobile robot application requirements (often Mbps range). For instance, real-time control, high-fidelity environmental mapping, and video streaming in advanced mobile robot and Industrial IoT (IIoT) scenarios typically demand throughputs in the megabits per second (Mbps) to gigabits per second (Gbps) range [15]. Limited downlink throughput restricts complex instructions and high-volume data. The even lower uplink throughput severely limits sensor data volume and frequency, making real-time high-fidelity environmental scans, continuous video, or detailed telemetry impractical. This constrained throughput directly impacts the robot's ability to engage in advanced functionalities, suggesting the current link supports only low-bandwidth, non-time-critical tasks. Future enhancements must address underlying factors like wireless channel efficiency, data compression, and processing pipeline streamlining for more sophisticated and responsive operations.

IV. CONCLUSION

This paper successfully presented a mobile robot system for automated warehouses, integrating magnetic landmark navigation with a cloud-based IoT communication framework. The system effectively utilizes a 16-element magnetic sensor for precise path guidance and an intelligent conditional stopping mechanism. A secure, centralized communication architecture, leveraging Google Sheets and standard internet protocols (HTTPS/TLS, JSON), facilitates two-way data exchange. Experimental results showed a high average landmark detection success rate of 91.42%, confirming the system's reliability. While end-to-end communication latency was predictable, throughput analysis indicated current limitations for high-bandwidth real-time applications. Future work should prioritize optimizing communication efficiency through enhanced wireless channels and data compression, alongside developing more dynamic path planning and obstacle avoidance capabilities, to enable sophisticated robotic operations.

REFERENCES

[1] P. K. Singh and A. G. S. Rao, "Task Scheduling with Mobile Robots—A Systematic Literature Review," MDPI, vol. 14, no. 6, p. 75, 2025.

[2] B. T. S. N. Banyu Tresno S.N, M. Ridwan, T. Kurniawaty, Y. Dinar, and V. Hartati, "DESIGN OF AUTOMATED GUIDED VEHICLE SYSTEM (mobile robot) FOR MATERIAL HANDLING IN FLEXIBLE MANUFACTURING SYSTEM (FMS)," Turkish Journal of Physiotherapy and Rehabilitation, vol. 32, no. 3, 2021, pp. 6397–6403.

[3] U. Jahn et al., "A Taxonomy for Mobile Robots: Types, Applications, Capabilities, Implementations, Requirements, and Challenges," Robotics, vol. 9, no. 4, p. 109, 2020, doi: 10.3390/robotics9040109.

[4] Z. Li et al., "Indoor Positioning Systems of Mobile Robots: A Review," MDPI, vol. 12, no. 2, p. 47, 2023.

[5] L. Zeng, S. Guo, J. Wu, dan B. Markert, "Autonomous mobile construction robots in built environment: A comprehensive review," Developments in the Built Environment, vol. 19, p. 100484, 2024, doi: 10.1016/j.dibe.2024.100484.

[6] T. Wang et al., "Research on Stability Design of Differential Drive Fork-Type mobile robot Based on PID Control," Electronics, vol. 9, no. 1072, pp. 1–18, 2020, doi: 10.3390/electronics9071072.

[7] B. R. Benni et al., "Automated Guided Vehicle (mobile robot)," International Journal of Research Publication and Reviews, vol. 5, no. 5, pp. 5858–5864, Mei 2024.

[8] T. S. Nguyen and A. S. Y. Lai, "Cloud Robotics: A Survey," IEEE Transactions on Industrial Informatics, vol. 12, no. 1, pp. 385-397, Feb. 2016.

[9] K. M. A. Kabir and M. R. M. N. Kabir, "Cloud Robotics for Enhancing Mobile Robot Capabilities," 2018 4th International Conference on Computing and Communications (ICCC), Dhaka, Bangladesh, 2018, pp. 1-6.

[10] V. Hernandez and J. M. I. de la Cruz, "Communication Architectures for Multi-Robot Systems: A Survey," Sensors, vol. 22, no. 1, p. 110, Jan. 2022.

[11] F. G. Cabral, G. S. R. L. R. P. Cabral and A. M. H. S. F. P. Cabral, "A survey on communication architectures for multi-robot systems," Robotics and Autonomous Systems, vol. 147, p. 103893, Jan. 2022.

[12] Q. Zeng, Z. Wang, Y. Zhou, H. Wu, L. Yang, and K. Huang, "Knowledge-Based Ultra-Low-Latency Semantic Communications for Robotic Edge Intelligence," arXiv preprint arXiv:2409.13319, 2024.

[13] M. Zolanvari, M. A. Sharafat, and S. C. Mukhopadhyay, "Recent Technologies, Security Countermeasure and Ongoing Challenges of Industrial Internet of Things (IIoT): A Survey," Sensors, vol. 21, no. 19, p. 6647, Oct. 2021, doi: 10.3390/s21196647.

[14] W. Boonsong, T. Inthasuth, and U. Kannan, "The Quality of RF Signal Communication Performance of LoRa-RSSI Analysis Based

on Various Environments Tests," International Journal of Electrical and Computer Engineering (IJECE), vol. 14, no. 3, pp. 2977-2985, Jun. 2024.

[15] V. A. M. H. V. Santos, A. K. F. L. L. Ribeiro, and R. P. F. L. Silva, "Real-Time Performance of Industrial IoT Communication Technologies: A Review," Proceedings of the 2017 IEEE International Conference on Industrial Technology (ICIT), pp. 1656-1661, 2017.